Water Science & Technology

IWA PUBLISHING

Water Science & Technology Vol 89 No 7, 1682 doi: 10.2166/wst.2024.098

Ascorbic acid enhanced the circulation between Fe(II) and Fe(III) in peroxymonosulfate system for fluoranthene degradation

Longbin Zhang, Jianxiong Gao, Yulong Liu, Zhengyuan Zhou, Xianxian Sheng, Dexiao Li, Yuantian Chen and Shuguang Lyu*

State Environmental Protection Key Laboratory of Environmental Risk Assessment and Control on Chemical Process, East China University of Science and Technology, Shanghai 200237, China
*Corresponding author. E-mail: lvshuguang@ecust.edu.cn

ABSTRACT

In this research, ascorbic acid (AA) was used to enhance Fe(II)/Fe(III)-activated permonosulfate (PMS) systems for the degradation of fluoranthene (FLT). AA enhanced the production of ROS in both PMS/Fe(II) and PMS/Fe(III) systems through chelation and reduction and thus improved the degradation performance of FLT. The optimal molar ratio in PMS/Fe(II)/AA/FLT and PMS/Fe(III)/AA/FLT processes were 2/2/4/1 and 5/10/5/1, respectively. In addition, the experimental results on the effect of FLT degradation under different groundwater matrixes indicated that PMS/Fe(III)/AA system was more adaptable to different water quality conditions than the PMS/Fe(II)/AA system. $SO_4^{\bullet-}$ was the major reactive oxygen species (ROS) responsible for FLT removal through the probe and scavenging tests in both systems. Furthermore, the degradation intermediates of FLT were analyzed using gas chromatograph-mass spectrometry (GC-MS), and the probable degradation pathways of FLT degradation were proposed. In addition, the removal of FLT was also tested in actual groundwater and the results showed that by increasing the dose and pre-adjusting the solution pH, 88.8 and 100% of the FLT was removed for PMS/Fe(II)/AA and PMS/Fe(III)/AA systems. The above experimental results demonstrated that PMS/Fe(II)/AA and PMS/Fe(III)/AA processes have a great perspective in practice for the rehabilitation of FLT-polluted groundwater.

Key words: ascorbic acid, Fe(II), Fe(III), peroxymonosulfate, remediation

HIGHLIGHTS

- The effect of AA on the circulation between Fe(II) and Fe(III) in the PMS system was investigated.
- $SO_4^{\bullet-}$ was the primary ROS in PMS/Fe(II)/AA and PMS/Fe(III)/AA systems.
- The effect of actual groundwater matrixes on FLT removal was investigated.
- The possible degradation pathways of FLT were proposed.
- Effective degradation of FLT in actual groundwater was achieved.

GRAPHICAL ABSTRACT

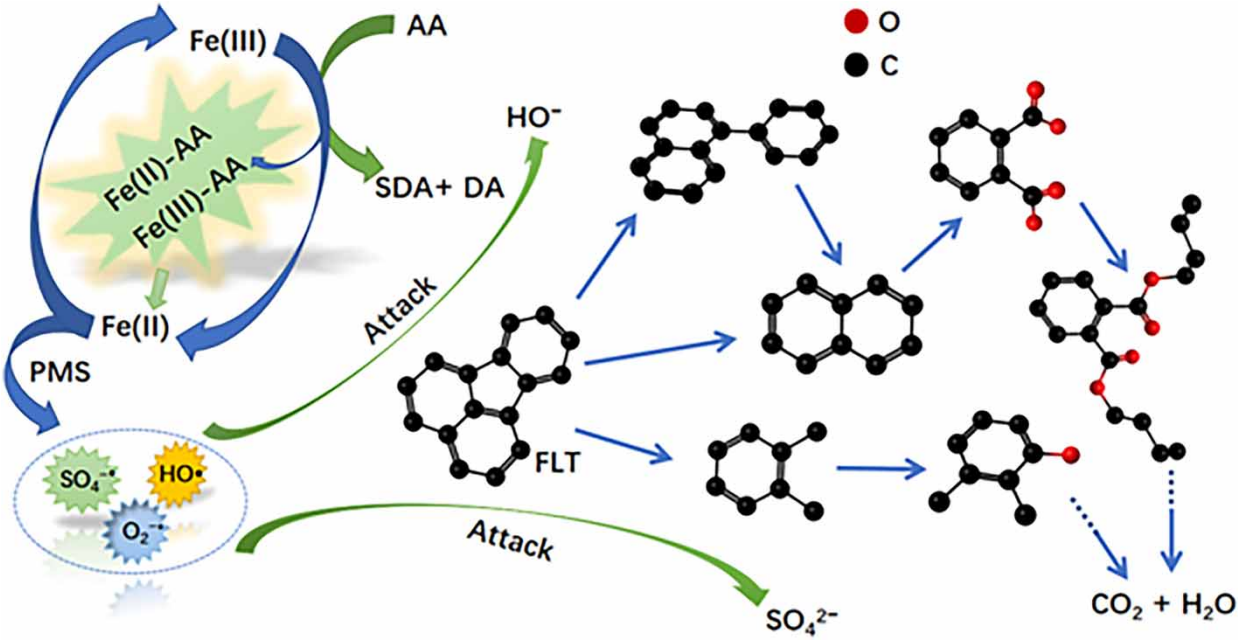

1. INTRODUCTION

Polycyclic aromatic hydrocarbons (PAHs) could be generated through industrial activities, energy production, and traffic exhausts, and enduringly exist in the soil of industrial sites and actual groundwater persistently. PAHs are getting more and more attention due to their complex composition, high concentration, and serious harm to the health of people. Fluoranthene (FLT) is frequently detected in contaminated sites in various countries as a typical PAH, which resulted in FLT being placed on the Environmental Protection Agency's (EPA) priority list for PAHs (Zhang & Chen 2017). FLT is mainly produced by incomplete combustion of organic matter and fossil fuels. As common PAHs, FLT has carcinogenic, teratogenic, and mutagenic properties, and most importantly, it is easily bio-accumulated and hard to biodegrade. FLT could enter the human body via breathing air containing FLT or by exposure to FLT-contaminated water and soil. In addition, FLT is photocytotoxic to human skin keratinocytes (Wang *et al.* 2007). Therefore, there is an urgent need to find an economic and efficient technology to restore FLT-contaminated groundwater and soil.

Currently, *in situ* chemical oxidation processes (ISCO) have been applied to degrade organic contaminants in contaminated soils and groundwater. It is reported that Fenton reagent, activated peroxydisulfate (PDS), activated peroxymonosulfate (PMS), O_3, and permanganate are widely used in ISCO (Sunder & Hempel 1997; Sutton *et al.* 2011; Lyu *et al.* 2020; Bein *et al.* 2023). PMS and PDS are more adoptable than other oxidants due to the broader pH application range, the less effect of soil moisture, and the longer duration of action in groundwater (Cheng *et al.* 2016). Both PMS and PDS are solid and soluble in water, and the aqueous solutions are acidic. The peroxide bond in PMS is asymmetric in charge distribution, inducing a partial positive charge on the peroxide oxygen attached to the hydrogen, whereas in PDS it is symmetrical, leading to the difference in reactivity between PMS and PDS. Several studies have shown that the groundwater component fraction has less effect on the activation of PMS compared to PDS (Wang & Wang 2018).

Metal ions (Fe, Cu, Mn, and Ru) and metal oxides are widely used to activate PMS to remove organic pollutants (Anipsitakis & Dionysiou 2004; Li *et al.* 2018a, 2018b; Lim *et al.* 2019). In this study, Fe(II) and Fe(III) were selected as activators of PMS because of their environmentally friendly properties, and reactive oxygen species (ROS) can be produced during the activation of PMS. As shown in Equations (1)–(3), it is worth noting that along with PMS activation by Fe(II) in producing $SO_4^{\bullet -}$ and $HO^{\bullet}$, $O_2^{\bullet -}$ is also produced in the PMS system (Zou *et al.* 2013; Cao *et al.* 2019). However, since excess Fe(II) also acts as a scavenger of the formed radicals (Equations (4) and (5)), the addition of Fe(II) needs to be appropriate (Zou *et al.* 2013). Fe(II) is converted to Fe(III) after the activation of PMS, and the redundant Fe(III) in solution converts a precipitated Fe(III) species ($Fe(OH)_3$), and further causes PMS activation ineffective (Dong *et al.* 2021). As

shown in Equations (1) and (6), the reaction constant of Fe(III) with HSO_5^- is only 3.0×10^{-9} M^{-1} s^{-1}, and it is tiny and 10^{13} times lower than that of Fe(II) with HSO_5^-, which is the reason for the ineffective activation of PMS by Fe(III) (Zou *et al.* 2013). It is reported that Fe(III) could be reduced by electrochemicals and significantly enhance the activation of PMS, because the reduction reaction can promote electron transport to Fe(III) to convert Fe(II) (Long *et al.* 2022). Thus, it is inevitable to choose a reduction means to eliminate the negative effect of Fe(III).

$$HSO_5^- + Fe(II) \rightarrow SO_4^{\bullet -} + HO^- + Fe(III)\ k = 3.0 \times 10^4\ M^{-1}s^{-1} \quad (1)$$

$$HSO_5^- + Fe(II) \rightarrow SO_4^{2-} + HO^{\bullet} + Fe(III) \quad (2)$$

$$Fe(II) + O_2 \rightarrow Fe(III) + O_2^{\bullet -} \quad (3)$$

$$Fe(II) + SO_4^{\bullet -} \rightarrow Fe(III) + SO_4^{2-}\ k = 3.0 \times 10^8\ M^{-1}\ s^{-1} \quad (4)$$

$$Fe(II) + HO^{\bullet} \rightarrow Fe(III) + HO^- \quad (5)$$

$$HSO_5^- + Fe(III) \rightarrow SO_5^{\bullet -} + H^+ + Fe(II)\ k = 3.0 \times 10^{-9}\ M^{-1}\ s^{-1} \quad (6)$$

Ascorbic acid (AA) is a ubiquitous vitamin found in various foods, particularly in plants and fruits. Due to its enediol structure conjugating with the carbonyl group in the lactone ring (Figure S1), it is also an important antioxidant, which plays a crucial role in inhibiting oxidative-induced cellular damage in both plant and animal tissues (Roig *et al.* 1993). AA is oxidated to non-toxic oxidation products such as hemihydro-L-ascorbate radical (SDA) and dehydro-L-ascorbate (DA) (Tripathi *et al.* 2009). AA is widely used in the reduction of metal activators in advanced oxidation processes. For example, some researchers have introduced AA into the H_2O_2/Cu(I) system to promote the Cu(I)/Cu(II) cycle in the system to improve the removal efficiency of pollutants (Zhou *et al.* 2016). Besides, the solution showed acidic properties with the addition of AA, which inhibited the iron precipitation and maintained the soluble iron stable (Roig *et al.* 1993). Importantly, iron chelates were formed after the addition of AA, in which Fe(II) was released more slowly with the generation of more stable chelated ions (Davies 1992).

Hence, in this study, AA was added to increase FLT removal by AA chelation with Fe(II) and Fe(III) in PMS/Fe(II) and PMS/Fe(III) processes. The outcomes of this study can provide efficient techniques for the remediation of FLT-contaminated groundwater. The purpose of this research was (1) to reveal the efficiency of FLT removal in PMS/Fe(II)/AA and PMS/Fe(III)/AA processes; (2) to demonstrate the major ROS for FLT degradation in both systems through the probe and scavenging experiments; (3) to investigate the effects of groundwater matrices and chemical agent dosage on FLT removal; (4) to propose the possible removal pathways of FLT based on the detected intermediates; and finally (5) to test the practicality of both systems for FLT removal in actual groundwater.

2. MATERIALS AND METHODS

2.1. Materials

Details of the chemical agents used in this study can be found in the supplementary material (Text S1).

2.2. Experimental procedures

All tests were performed in the glass reactor (250 mL) with stirring at 700 r min^{-1}. The RPM used in this study was intended to make full contact with contaminants (FLT) between chemical agents added to the reactor so that the process of FLT removal could be performed quickly and efficiently. The treatment method used in this study has been adopted in several studies, and it can even reach 800 rpm (Cheng *et al.* 2016; Cao *et al.* 2019; Li *et al.* 2019a; Xu *et al.* 2022). Firstly, 0.004 M FLT stock solution was prepared with 0.02 g FLT dissolving in acetone (25 mL). Then, 1.0 μM FLT-contaminated solution was prepared by adding 0.248 mL of FLT stock solution in 1.0 L of ultrapure water, and the mixture was stirred for 9 h to ensure the sufficient dissolution of FLT. The reasons for the choice of acetone and the description of the stability of the aqueous FLT solution are given in Text S4. Two hundred and fifty mL FLT-contaminated solution was transferred into the reactor where only 0.062 mL acetone was presented, and the ratio of acetone to water was about 1/4,000, hence the influence of acetone on ROS was negligible. In addition, other predetermined dosage reagents (Fe(II), Fe(III), and AA) were added successively. Finally, PMS was added to start the test. At the desired time, 0.7 mL of the sample was removed into

a brown vial (4 mL) containing 0.7 mL of methanol (stopping the reaction). After that, the samples were filtered through 0.22 μm microporous organic filters before analyzing the FLT concentration by high-performance liquid chromatography (HPLC). The reactions were performed three times at least and the results were averaged.

To investigate the influence of the pH of aqueous solution in both systems, the aqueous initial solution pH was adjusted to 2.0, 3.0, 5.0, 7.0, 9.0, and 11 by 0.1 M H_2SO_4 and 0.1 M NaOH. It is reported that the inorganic anions (Cl^-, Br^-, and HCO_3^-) broadly exist in natural water and groundwater, which could influence FLT removal in both systems (Carol & Alvarez 2016). Several representative inorganic anions (Cl^-, Br^-, and HCO_3^-) were selected to investigate the effect of inorganic anions on FLT removal, and the concentrations were set as 1.0, 20, and 50 mM based on the concentration present at the actual contaminated site (Carol & Alvarez 2016).

Natural organic matter (NOM) existing in actual groundwater could react with $SO_4^{\bullet-}$ and $HO^\bullet$ and further influence the removal of contaminants (Li *et al.* 2019b). Therefore, the effect of humic acid (HA) on FLT removal in PMS/Fe(II)/AA and PMS/Fe(III)/AA systems was investigated. Considering the concentrations of HA substances in groundwater, the chemical dosages of HA were set to 1.0, 3.0, 5.0, 10, 50, and 100 mg L^{-1} in the test to explore the influence of HA for FLT removal (Li *et al.* 2019c).

The specific scavengers were first added to the aqueous solution containing FLT in the scavenging experiments, and then other chemicals were added to initiate the reaction (the reaction rate constants of different scavengers with ROS are shown in Text S3). The dominant ROS in PMS/Fe(II)/AA and PMS/Fe(III)/AA processes were determined based on the degradation of FLT with the addition of different scavengers. In electron paramagnetic resonance (EPR) tests, 5,5-dimethyl-1-oxypyrrolidine (DMPO) was used as the ROS trap to detect the presence of different ROS. At the reaction time of 2.0 min, the 1.0 mL sample was added to a 4.0 mL vial pre-filled with 1.0 mL aqueous DMPO solution, and the mixture was analyzed by EPR.

In the probe experiments, degradation experiments were performed with probe compounds instead of FLT to investigate the types of reactive radicals in both systems. Since nitrobenzene (NB) has a high reactivity with $HO^\bullet$ ($k_{HO\cdot} = 3.9 \times 10^9\ M^{-1}\ s^{-1}$) and is more reactive than with $SO_4^{\bullet-}$, the reaction rate constant is three orders of magnitude higher, while $O_2^{\bullet-}$ hardly reacts with NB, so NB was chosen as the chemical probe for $HO^\bullet$ (Buxton *et al.* 1988). The rate constant for the reaction of carbon tetrachloride (CT) with $O_2^{\bullet-}$ ($1.6 \times 10^{10}\ M^{-1}\ s^{-1}$) is higher than that of $HO^\bullet$ ($k_{HO\cdot} < 2 \times 10^6\ M^{-1}\ s^{-1}$), and therefore CT was chosen as the chemical probe for $O_2^{\bullet-}$ in this experiment (Ahmad *et al.* 2015). Since all chemicals that can react with $SO_4^{\bullet-}$ can react with $HO^\bullet$, a separate probe suitable for $SO_4^{\bullet-}$ could not be selected (Teel & Watts 2002). The reaction rate constants of anisole (AN) with $SO_4^{\bullet-}$ and $HO^\bullet$ are all greater than $10^9\ M^{-1}\ s^{-1}$, AN was chosen as both $HO^\bullet$ and $SO_4^{\bullet-}$ probe (Ahmad *et al.* 2012).

2.3. Analytical methods

The concentrations of FLT were detected through HPLC (LC-20AT, Shimadzu, Japan), which set 235 nm as the detection wavelength and 30 °C oven temperature. The constituents of the HPLC mobile phase were 1:9 ratio of methanol and water. The injection volume of the sampler was 100 μL. Other significant analytical methods of the tests are exhibited in the supplementary material (Text S2).

3. RESULTS AND DISCUSSION

3.1. The effectiveness of FLT removal in PMS/Fe(II)/AA and PMS/Fe(III)/AA systems

The effect of FLT removal in various systems is shown in Figure 1(a) and 1(b), the molar ratio of PMS/Fe(II)/AA/FLT and PMS/Fe(III)/AA/FLT were 2/2/4/1 and 5/10/5/1. In the control group, it was revealed that 3.9% FLT was lost during the reaction due to the volatilization of FLT, suggesting that the effect of FLT natural evaporation was minimal in the entire reaction. Only 9.7 and 8.0% of FLT were removed when Fe(II) or Fe(III) were added individually without other agents. The degradations of FLT were 5.7 and 22.3% when AA or PMS were added individually. When PMS was only added without AA, 22.3% of FLT was removed, which was due to the fact that the unactivated PMS could also react directly with various compounds (Yang *et al.* 2018). Then, FLT was degraded by 5.7% when AA was added to the solution without other agents, and FLT was removed by 9.0 and 7.8% in Fe(II)/AA and Fe(III)/AA systems, respectively.

For the PMS/Fe(II)/AA process, FLT removal was merely 35.7% for the PMS/Fe(II) process, but the FLT degradation dramatically increased in the initial 5 min. It is worth noting that FLT removal increased significantly from 35.7 to 90.0% when AA was added to the PMS/Fe(II) process. For PMS/Fe(III)/AA process, when the molar ratios of PMS/Fe(III)/AA/FLT were set at 2/2/4/1, 5/5/10/1, and 5/10/10/1, the degradation of FLT was 57.6, 75.3, and 90.6%, respectively (Figure S3). Finally,

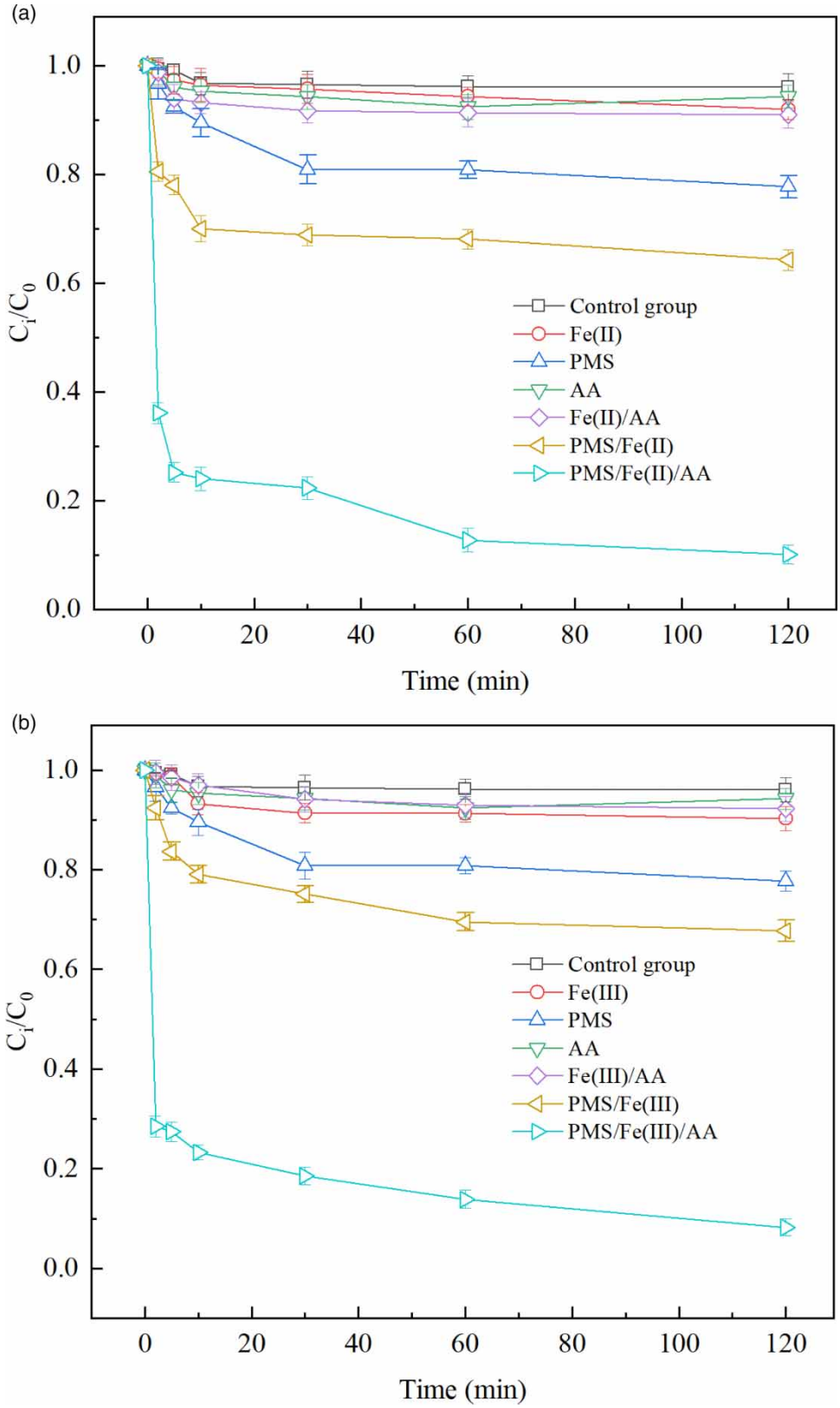

Figure 1 | FLT degradation performance detected by HPLC in (a) PMS/Fe(II)/AA system ($[FLT]_0 = 0.2$ mg L^{-1}, $[PMS]_0 = 5.0$ mg L^{-1}, $[Fe(II)]_0 = 2.0$ mg L^{-1}, and $[AA]_0 = 2.8$ mg L^{-1}) and (b) PMS/Fe(III)/AA system ($[PMS]_0 = 12$ mg L^{-1}, $[FLT]_0 = 0.2$ mg L^{-1}, $[Fe(III)]_0 = 11$ mg L^{-1}, and $[AA]_0 = 3.5$ mg L^{-1}).

in order to investigate the optimal AA dosage in this study, the molar ratio of PMS/Fe(III) was fixed to 5/10, FLT was removed by 91.8 and 87.7% for PMS/Fe(III)/AA process on the molar ratios of 5/10/5 and 5/10/20, respectively. The decrease of FLT degeneration with increasing molar ratio of AA was due to the scavenging effect of excess AA for ROS ($SO_4^{\bullet -}$ and $HO^{\bullet}$) (Xu *et al.* 2022). The degradation of FLT hardly changed after continuing to increase the amount of PMS based on the molar ratio of 5/10/5 for the PMS/Fe(II)/AA system. Therefore, 5/10/5 was chosen as the optimal molar ratio for the PMS/Fe(III)/AA system in this study considering the actual remediation cost and other factors.

The degradations of FLT were merely 32.3% for the PMS/Fe(III) system but increased to 91.8% with the addition of AA. For PMS/Fe(II)/AA process, PMS was rapidly activated by the addition of Fe(II) to produce free radicals due to their large reaction rate constants (Equation (1)). Therefore, the reaction of FLT removal is very fast within 10 min. Three different experimental operators were invited to perform the degradation experiments of FLT in different laboratories. As shown in Figure S2, the experimental results were almost the same as the previous results, which proved the good reproducibility of the experiments. In the PMS/Fe(III)/AA system, Fe(III) was first reduced to Fe(II) by AA, and then PMS was activated by the regenerated Fe(II) to produce various ROS and thus enhance the degradation of FLT. The PMS oxidative process became more sustained during the entire experiment period when AA was added, which proved that the addition of AA is extraordinarily effective for FLT degradation. There are many explanations for these phenomena. First, adding AA can decrease the solution pH, which could ensure sufficient Fe(II) in the solution by preventing the precipitation of iron. Second, AA is similar to citric acid (CA), which can chelate with metal ions (Thinh *et al.* 2021). AA can chelate iron with Fe(II) and Fe(III) in solution, which could prevent the precipitation of iron species, thus promoting the generation of ROS and the degradation of FLT (Zhou *et al.* 2016). In addition, the addition of AA could promote the redox cycle of Fe(III)/Fe(II) in the process due to the reduced ability of AA, which in turn would promote the production of ROS (Thinh *et al.* 2021). As shown in Figure 2, the concentration of Fe(II) in the reaction was significantly elevated by the addition of AA due to the reduction and chelation of AA compared with PMS/Fe(II) and PMS/Fe(II) processes.

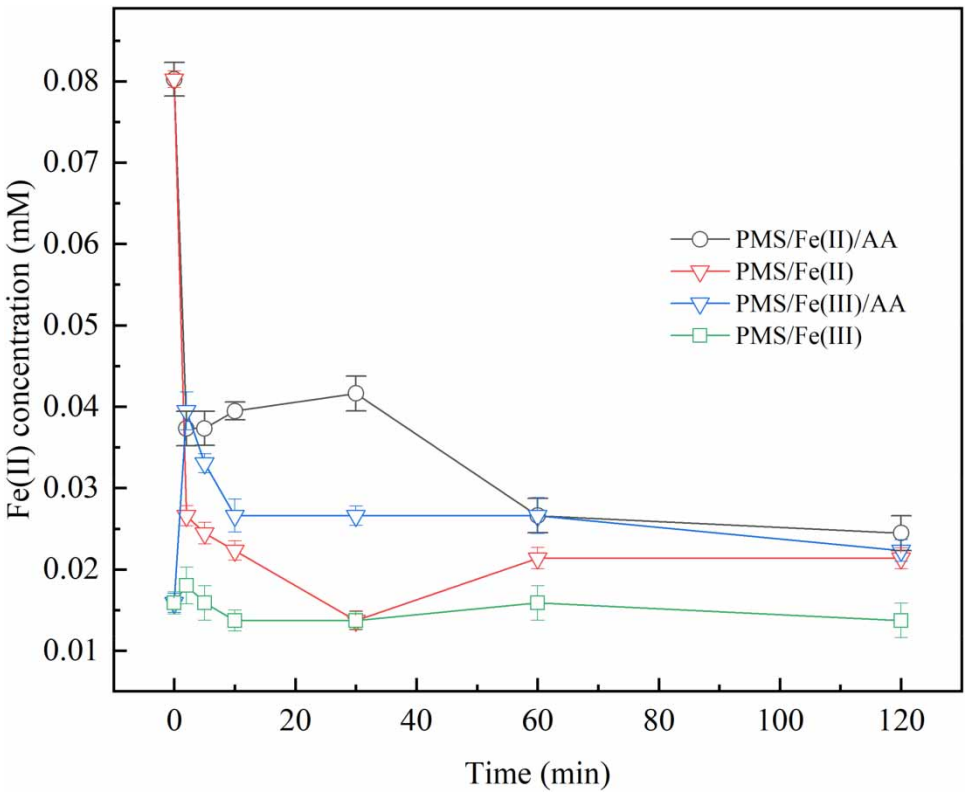

Figure 2 | Variation of Fe(II) concentration in PMS/Fe(II)/AA system and PMS/Fe(III)/AA system detected by *o*-phenanthroline spectrophotometry ($[FLT]_0 = 0.2$ mg L^{-1}, $[PMS]_0 = 0.08$ mM, $[Fe(II)]_0 = 0.08$ mM, and $[AA]_0 = 0.16$ mM; $[PMS]_0 = 0.1$ mM, $[Fe(III)]_0 = 0.2$ mM, and $[AA]_0 = 0.1$ mM).

The initial pH of PMS/Fe(II) and PMS/Fe(III) needed to be kept consistent with that of PMS/Fe(II)/AA and PMS/Fe(III)/AA processes with only Fe(II), Fe(III) and AA added to investigate whether the increase in FLT degradation was due to the influence of pH decrease or to the influence of reduction and chelation reactions after the addition of AA. The original solution pH of PMS/Fe(II) and PMS/Fe(III) processes was adjusted to 5.3 and 4.6 by 0.1 M H_2SO_4 which was consistent with the unadjusted pH of PMS/Fe(II)/AA and PMS/Fe(III)AA processes. As shown in Figure S4a and Figure S4b, the removal of FLT increased only 4.7 and 6.4% than the unadjusted one, confirming that the increase in FLT removal was mainly due to the chelation and reduction of iron by AA.

Previous studies have demonstrated the chelation reaction of AA with iron, showing that AA and Fe(III) form Fe(III)-AA chelates via an inner-sphere mechanism in milliseconds and also isolating a Fe(II)-AA chelate in the distorted octahedral environment realized in the polymeric structure (Kontoghiorghes *et al.* 2020). The full wavelength scan of UV-vis spectrum was used to investigate the chelating effect of AA (Ren *et al.* 2020). As shown in Figure S5, the characteristic absorption peak of AA was located at 253 nm. After the addition of Fe(II) and Fe(III), the characteristic absorption peak was red-shifted. In addition, after the addition of Fe(II), a new absorption band at 261–290 nm was formed, indicating that AA can chelate Fe(II). The absorption band at 261–648 nm shifted obviously and the intensity of the characteristic absorption peak increased significantly after the addition of Fe(III), which proved that AA has a strong chelating effect on Fe(III) compared with Fe(II).

Wu *et al.* (2015) investigated the degradation effects of hydroxylamine hydrochloride (HAH), sodium thiosulfate (STS), and sodium sulfite (SS) on trichloroethylene (TCE) removal in the peroxysulfate process and found that each reductant could promote the TCE removal. Li *et al*. (2019a) and Luo *et al.* (2021) also added HAH to the PMS/Fe(II) process to promote the Fe(II)/Fe(III) cycle by utilizing the reduction of HA, thus sufficiently activating the PMS to improve the pollutant removal rate increase. Rastogi *et al.* (2009a) investigated the effect of the different chelating agents (sodium citrate, sodium pyrophosphate, and ethylenediamine disuccinate (EDDS)) on the degradation of chlorophenols in the PMS system, and found that the pyrophosphate and EDDS chelated Fe(II) followed by slowly releasing Fe(II) to enhance the efficiency of activation of PMS (Rastogi *et al.* 2009a). Wu *et al.* (2014) also used CA-chelated Fe(II)-activated PDS to degrade TCE, and TCE could be degraded. In this research, the optimal molar ratio in PMS/Fe(II)/AA/FLT and PMS/Fe(III)/AA/FLT systems were 2/2/4/1 and 5/10/5/1, respectively, when the initial concentration of FLT was 1.0 μM. As shown in Table 1, The dosage of various

Table 1 | Comparative studies with other studies on iron-activated PMS and PDS systems

Process	Pollutant	Enhanced agent	Experimental conditions	Degradation efficiency	Ref.
PMS/Fe(II)/HAH	Benzoic acid (40 μM)	Hydroxylamine (HAH)	$[HAH]_0 = 0.40$ mM, $[Fe(II)]_0 = 10.8$ μM, $[PMS]_0 = 0.32$ mM	80% ($pH_0 = 3.0$)	Zou *et al.* (2013)
PDS/Fe(II)/HAH	Trichloroethylene (0.15 mM)	HAH	$[HAH]_0 = 1.5$ mM, $[Fe(II)]_0 = 3.0$ mM, $[PDS]_0 = 2.25$ mM	97.9% ($pH_0 = 4.0$)	Wu *et al.* (2015)
PMS/Fe_3O_4/HAH	Atrazine (23 μM)	HAH	$[HAH]_0 = 0.3$ mM, $[Fe_3O_4]_0 = 0.69$ g L^{-1}, $[PMS]_0 = 0.4$ mM	94% ($pH_0 = 6.8$)	Li *et al.* (2019a)
PMS/FeOCl/HAH	Ciprofloxacin (5.0 mg L^{-1})	HAH	$[HAH]_0 = 1.0$ mM, $[FeOCl]_0 = 0.2$ g L^{-1}, $[PMS]_0 = 1.5$ mM	74.5% ($pH_0 = 6.5$)	Luo *et al.* (2021)
PDS/Fe(II)/STS	Trichloroethylene (0.15 mM)	Sodium thiosulfate (STS)	$[STS]_0 = 1.5$ mM, $[Fe(II)]_0 = 3.0$ mM, $[PDS]_0 = 2.25$ mM	65.5% ($pH_0 = 5.5$)	Wu *et al.* (2015)
PDS/Fe(II)/SS	Trichloroethylene (0.15 mM)	Sodium sulfite (SS)	$[SS]_0 = 1.5$ mM, $[Fe(II)]_0 = 3.0$ mM, $[PDS]_0 = 2.25$ mM	81.1% ($pH_0 = 6.3$)	Wu *et al.* (2015)
PMS/Fe(II)/Citrate	4-chlorophenols (0.396 mM)	Citrate	$[citrate]_0 = 0.4$ mM, $[Fe(II)]_0 = 0.99$ mM, $[PMS]_0 = 3.96$ mM	27.0% ($pH_0 = 7.0$)	Rastogi *et al.* (2009a)
PMS/Fe(II)/EDDS	4-chlorophenols (0.396 mM)	Ethylenediaminedisuccinate (EDDS)	$[EDDS]_0 = 0.4$ mM, $[PMS]_0 = [Fe(II)]_0 = 0.99$ mM	91.5% ($pH_0 = 7.0$)	Rastogi *et al.* (2009a)
PMS/Fe(II)/Pyro	4-chlorophenols (0.396 mM)	Pyrophosphate (Pyro)	$[Pyro]_0 = 0.40$ mM, $[Fe(II)]_0 = 0.99$ mM, $[PMS]_0 = 3.96$ mM	91.5% ($pH_0 = 7.0$)	Rastogi *et al.* (2009a)
PDS/Fe(II)/CA	Trichloroethylene (0.15 mM)	Citric acid (CA)	$[CA]_0 = 0.15$ mM, $[Fe(II)]_0 = 3.0$ mM, $[PDS]_0 = 2.25$ mM	100% ($pH_0 = 4.0$)	Wu *et al.* (2014)

agents for the different enhancement systems was significantly higher than in the present study since the addition of AA has both the reducing and chelating effect. In conclusion, AA was an efficient and economically enhanced agent in the persulfate system.

3.2. Influence of concentration (PMS, Fe(II), Fe(III), and AA) on FLT removal

3.2.1. Influence of PMS concentration

The initial concentrations of Fe(II), AA, and FLT were set at 2.0, 2.8, and 0.2 mg L^{-1}, respectively, while changing the dosage of PMS from 2.0 to 40 mg L^{-1}. Figure S6a shows that FLT removal was increased from 85.0 to 100% with the dosage of PMS increasing from 2.0 to 10 mg L^{-1}, which suggested that an appropriate concentration of PMS can generate more ROS and improve FLT removal. However, FLT removal decreased to 81.1% with further increasing the dosage of PMS to 40 mg L^{-1}, which indicated that the dosage of PMS was not proportional to the degradation of FLT.

The concentrations of Fe(III), AA, and FLT were set to 11, 3.5, and 0.2 mg L^{-1} in the PMS/Fe(III)/AA system, respectively, while changing the dosage of PMS from 5 to 96 mg L^{-1}. Figure S6b shows FLT removal was increased from 71.8 to 95.1% with an increase in the dosage of PMS from 5.0 to 48 mg L^{-1}. Similar to the PMS/Fe(II)/AA process, the degradation of FLT barely changed in the PMS/Fe(III)/AA process when the concentration of PMS further increased to 96 mg L^{-1}. It could be due to the decrease of ROS caused by the reaction of excess PMS with ROS. The amount of $SO_4^{\bullet-}$ in the solution also kept increasing with the addition of excess PMS, but the excess $SO_4^{\bullet-}$ reacted with itself, $HO^{\bullet}$ and HSO_5^-, and $HO^{\bullet}$ could also react with HSO_5^- (Equations (7)–(10)) (Zou *et al.* 2013). Cao *et al.* (2019) found that $SO_4^{\bullet-}$ was further consumed by itself when the concentration of PMS was excessive in investigating the effect of the Fe(0)/PMS process on tetracycline (TC) removal, which resulted in the degradation of TC decrease insignificantly with the increase of PMS:

$$SO_4^{\bullet-} + HO^{\bullet} \rightarrow HSO_4^- + 1/2O_2 \quad (7)$$

$$SO_4^{\bullet-} + SO_4^{\bullet-} \rightarrow S_2O_8^{2-} \quad (8)$$

$$HSO_5^- + SO_4^{\bullet-} \rightarrow SO_4^- + SO_5^{\bullet-} + H^+ \quad (9)$$

$$HSO_5^- + HO^{\bullet} \rightarrow SO_5^{\bullet-} + H_2O \quad (10)$$

3.2.2. Effect of Fe(II)/Fe(III) dosage

For PMS/Fe(II)/AA process, as illustrated in Figure S7a, with Fe(II) concentrations increasing to 4 mg L^{-1}, FLT removal enhanced to 91.1% when PMS, AA, and FLT were set as 5.0, 2.8, and 0.2 mg L^{-1}, respectively. It proved that PMS was activated efficiently to strengthen the production of ROS in the solution following the appropriate increase in Fe(II) concentration. However, the FLT removal was decreased to 38.7% when Fe(II) dosage was sequentially increased to 16 mg L^{-1}.

For the PMS/Fe(III)/AA process, with the concentrations of Fe(III) increasing from 6.0 to 22 mg L^{-1}, FLT removal increased from 80.5 to 96.3% when PMS, AA, and FLT were set to 12, 3.5, and 0.2 mg L^{-1} in Figure S7b, respectively. It was similar to Fe(II) in that the degradation of FLT barely changed when the concentrations of Fe(III) further increased to 88 mg L^{-1}. For the PMS/Fe(II)/AA process, the excess Fe(II) could consume $SO_4^{\bullet-}$ and $HO^{\bullet}$ by the reaction of Fe(II) and ROS (Equations (4) and (5)), which can inhibit the degradation of FLT (Rastogi *et al.* 2009a). For the PMS/Fe(III)/AA process, the excess Fe(III) was first reduced to Fe(II) by AA, and the resulting Fe(II) was identical to the PMS/Fe(II)/AA process, which can act as a scavenger for free radicals. Xu *et al.* (2022) explored the influence of Fe(0) concentration on benzoic acid (BA) removal in the AA/Fe(0)/PMS process and found that appropriately increasing the dosage of Fe(0) could promote the degradation of BA, but the BA removal remained unchanged in the excess of Fe(0), which was attributed to the fact that the excess of Fe(II) scavenged the free radicals in the system. Rastogi *et al.* (2009b), in studying the effect of polychlorinated biphenyls (PCBs) removal Fe(II)/PMS process, found that the higher concentration of Fe(II) scavenged the free radicals and thus inhibited PCBs removal. The results of these experiments indicated that for both systems, the appropriate amount of iron was necessary for the effective activation of PMS.

3.2.3. Effect of AA concentration

For PMS/Fe(II)/AA process, the concentrations of PMS, Fe(II), and FLT were set to 5.0, 2.0, and 0.2 mg L^{-1}, respectively. With the dosage of AA increasing from 0 to 2.8 mg L^{-1}, FLT removal enhanced from 35.7 to 90.0%, as shown in

Figure S8a. Fe(III) produced after Fe(II) oxidated was reduced by AA to restrict the precipitation of iron and continue activating PMS, which could explain why the degradation of FLT increased after AA was added. However, FLT removal decreased to 68.9% when the dosage of AA was increased to 5.6 mg L^{-1}.

For the PMS/Fe(III)/AA process, the dosages of PMS, Fe(III), and FLT were set to 12, 11, and 0.2 mg L^{-1}, respectively. The degradation of FLT increased from 32.3 to 91.8% with increasing the dosage of AA from 0 to 3.5 mg L^{-1} in Figure S8b. However, FLT removed only 30.8% when the dosage of AA was increased to 28 mg L^{-1}. This phenomenon indicated that FLT removal was not proportional to the dose of AA because AA could react with $SO_4^{\bullet-}$ and $HO^{\bullet}$ causing unnecessary consumption (Equations (11) and (12)) based on the previous research (Xu *et al.* 2022). Li *et al.* (2023) reported that AA could be degraded along with sulfadimethoxine (SMT) in the iron silicate composite (ISC)/PDS/AA process, and the degradation intermediates of both AA and SMT were examined by liquid chromatograph–mass spectrometry (LC-MS). It was noted that AA was ultimately converted to a green, non-toxic substance in the ISC/PDS/AA process based on the detected degradation intermediates of AA, indicating that the addition of AA was environmentally friendly. In this research, $SO_4^{\bullet-}$ and $HO^{\bullet}$ were the dominant ROS both in PMS/Fe(II)/AA and PMS/Fe(III)/AA systems, but FLT removal was significantly enhanced by AA both in PMS/Fe(II) and PMS/Fe(III) systems (Figure 1). Thus, it can be speculated that AA could react with ROS ($SO_4^{\bullet-}$ and $HO^{\bullet}$) during FLT removal, but the consumption of ROS by AA was negligible. In consequence, the addition of appropriate AA dosage is very important in practical applications. In this study, the optimal molar ratio was 2/2/4 and 5/10/5 for PMS/Fe(II)/AA and PMS/Fe(III)/AA processes, respectively:

$$H_2A\ (AA) + SO_4^{\bullet-} \rightarrow SO_4^{2-} + A^{\bullet-} + 2H^+ \quad (11)$$

$$H_2A\ (AA) + HO^{\bullet} \rightarrow H_2O + A^{\bullet-} + H^+ \quad (12)$$

3.3. The mechanisms of FLT removal in PMS/Fe(II)/AA and PMS/Fe(III)/AA processes

3.3.1. Detecting ROS by the tests of probe and EPR

It is reported that a variety of ROS ($SO_4^{\bullet-}$, $HO^{\bullet}$, and $O_2^{\bullet-}$) could be produced in the PMS/Fe(II) process, which could be also produced in PMS/Fe(II)/AA and PMS/Fe(III)/AA processes as well (Dong *et al.* 2021). Anisole was chosen as both $SO_4^{\bullet-}$ and $HO^{\bullet}$ probe compounds, CT and nitrobenzene were chosen as $O_2^{\bullet-}$, and $HO^{\bullet}$ probe compounds to confirm the generated ROS in the process (Ahmad *et al.*, 2012, 2015). In Figure S9a, CT removal indicated the presence of $O_2^{\bullet-}$. Figure S9b shows the presence of HO· because of NB removal. AN was also removed with the addition of excess tertiary butyl alcohol (TBA), which proved the existence of $SO_4^{\bullet-}$ in both processes (Figure S9c and S9d). In addition, the addition of AA could increase NB, AN, and CT removal, confirming AA can promote the production of ROS.

In this study, the presence of ROS was further demonstrated through EPR testing in both systems. In Figure S10a and Figure S10b, it indicated the presence of $SO_4^{\bullet-}$ and $HO^{\bullet}$ because of the formation of DMPO-OH and DMPO-SO_4 adducts. However, the peaks of adducts composed (DMPO and $O_2^{\bullet-}$) were not detected because of the low stability and concentration of $O_2^{\bullet-}$ (Fang *et al.* 2013).

3.3.2. The role of ROS in FLT degradation

Isopropanol (IPA), chloroform (CF), and TBA acted as the scavengers for $SO_4^{\bullet-}$ and $HO^{\bullet}$, $O_2^{\bullet-}$, and $HO^{\bullet}$, respectively. The reaction constants of different scavengers with various ROS are shown in the supplementary material (Text S3). For PMS/Fe(II)/AA and PMS/Fe(III)/AA processes, as shown in Figure 3(a) and 3(b), FLT was removed by 90.0 and 91.8% without scavengers, respectively, but it drastically decreased to 31.2 and 27.1% when IPA was added, which suggested that $SO_4^{\bullet-}$ was the predominant ROS on FLT removal. Notably, compared with the scavenger-free experiment (90.0 and 91.8%), FLT removal was decreased by 11.1 and 17.9% when TBA was added, indicating the major role of $HO^{\bullet}$ on FLT degradation. Finally, FLT removal was also restricted when the excess CF was added, which elucidated $O_2^{\bullet-}$ also suggested FLT degradation. Therefore, the above results indicated that the contribution of $O_2^{\bullet-}$ and $HO^{\bullet}$ for the FLT removal was much lower than the $SO_4^{\bullet-}$ attributed to in both processes. The initial pH of the solution was 5.4 (FLT contamination solution). At acidic pH (3.0–6.0), both $SO_4^{\bullet-}$ and $HO^{\bullet}$ exhibited similar reduction potentials (Chan & Chu 2009). These two radicals have different oxidizing abilities at neutral pH and similar oxidizing abilities at acidic pH. However, $SO_4^{\bullet-}$ exhibits a higher standard redox potential (2.5–3.1 V) at neutral pH compared to $HO^{\bullet}$ (1.9–2.7 V). Besides, the experimental results

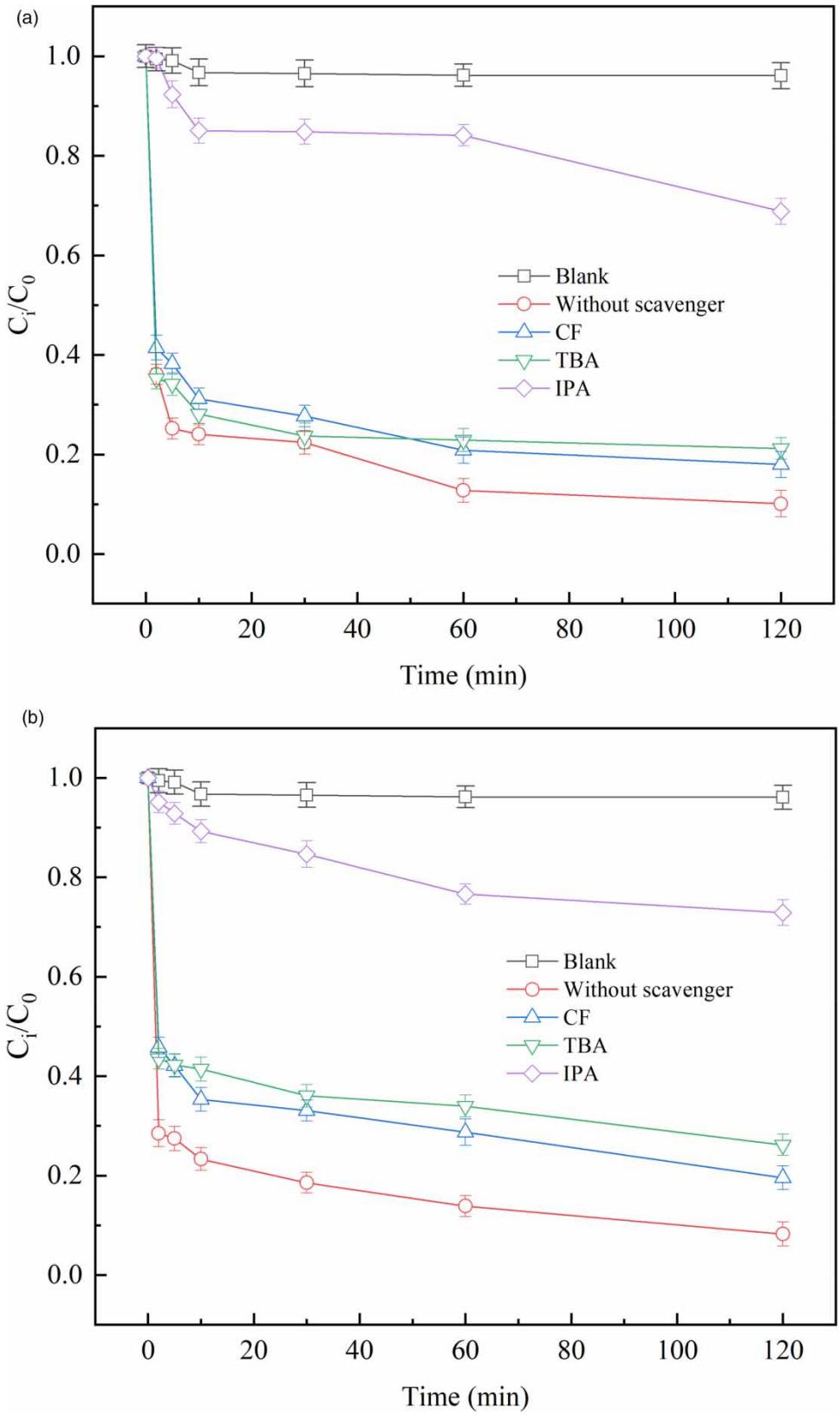

Figure 3 | Effect of scavengers on FLT degradation detected by HPLC in (a) PMS/Fe(II)/AA system ($[IPA]_0 = [TBA]_0 = [CF]_0 = 10$ mM, $[FLT]_0 = 0.2$ mg L^{-1}, $[PMS]_0 = 5.0$ mg L^{-1}, $[Fe(II)]_0 = 2.0$ mg L^{-1}, and $[AA]_0 = 2.8$ mg L^{-1}) and (b) PMS/Fe(III)/AA system ($[IPA]_0 = [TBA]_0 = [CF]_0 = 10$ mM, $[PMS]_0 = 12$ mg L^{-1}, $[FLT]_0 = 0.2$ mg L^{-1}, $[Fe(III)]_0 = 11$ mg L^{-1}, and $[AA]_0 = 3.5$ mg L^{-1}).

in this research show that FLT can react effectively with $SO_4^{\bullet-}$ (Section 3.1 and 3.3.2). In general, $SO_4^{\bullet-}$ was more selective for the oxidation of FLT than for the oxidation of $HO^{\bullet}$ (Chan & Chu 2009).

3.4. Influence of water quality conditions on FLT degradation

3.4.1. Effect of aqueous solution pH

For the PMS/Fe(II)/AA system, FLT was removed 58.0, 77.6, 93.4, 82.6, 51.6, and 45.6% with the pH of reaction solution pre-adjusting to 2.0, 3.0, 5.0, 7.0, 9.0, and 11 in Figure S11a, respectively. For PMS/Fe(III)/AA system, the degradations of FLT were 88.2, 100.0, 100.0, 98.0, 89.1, and 19.2% with the aqueous solution pH increasing from 2.0 to 3.0, 5.0, 7.0, 9.0 and 11 in Figure S11b, respectively. The above results show that FLT can be effectively removed for both systems when the initial pH of the solution was 3.0–9.0. FLT could be efficiently degraded under acidic conditions because it could increase the production of sulfate radicals that are more stable and can induce iron dissolution to benefit the Fenton-like oxidation (Pignatello *et al.* 2006). However, the degradations of FLT decreased at an initial solution pH of 2.0, which proved that the extremely acidic condition was unfavorable to FLT removal. There were explanations for this phenomenon. At extreme acidic pH, AA existed mainly in the protonated form, which was not conducive to chelated iron production (Torres *et al.* 1982). What is more, the lower efficiency of FLT removal was also attributed to the generation of the iron complex species ($[Fe(H_2O)_6]^{2+}$), which was slower to react with PMS than other Fe(II) species (Xu *et al.* 2009).

In addition, FLT was removed unsatisfactorily in the alkaline environment. In the first place, more stable chelated ferrous ions formed by increasing the solution pH, which was unfavorable for Fe(II) release and thus led to the failure of PMS activation (Davies 1992). Then, Fe(II) and Fe(III) were precipitated at a high pH of the solution, reducing the concentration of dissolved Fe(II) and thus limiting the activation of the PMS. Furthermore, $SO_4^{\bullet-}$ will be consumed by reacting with OH^- under alkaline conditions (Yuan *et al.* 2011), which was the dominant radical for FLT degradation. Finally, AA was decomposed in the alkaline condition, which caused the significant decrease of chelated iron ions and the failure of reduction (Munialo & Kontogiorgos 2014). Munialo and Kontogiorgos (2014) conducted a kinetic study on the decomposition of AA at different solution pH values and indicated that in the aqueous solution, there was an equilibrium between AA and the oxidized product dehydroascorbic acid (DHAA), but increasing solution pH favored the transformation DHAA from AA, which caused the increase of AA decomposition. Tu *et al.* (2017) investigated the scavenging action of AA on free radicals and discovered that AA performed disproportionation reactions due to internal electron transfer at pH 7.

As shown in Figure S11, the solution pH changed significantly before and after the reaction at the initial pH of 7.0 and 9.0, so further experiments were conducted to investigate the change in solution pH with time after adding the agents. Figure S12 demonstrates that the solution pH decreased rapidly within 10 min after the addition of the agent and then stabilized, which was due to the acidic nature of the added PMS. In conclusion, the performance of FLT removal was better under acidic conditions, and by comparison, the PMS/Fe(III)/AA system was more adaptable to pH changes than the PMS/Fe(II)/AA system. On the one hand, this could be since the hydrolysis of Fe(III) can produce H^+ to lower the pH, thus reducing the influence of the initial pH. On the other hand, this was because the results of chelation experiments in AA with iron showed the strong chelating effect of AA on Fe(III) compared to Fe(II) (Figure S5), thus preventing the rapid precipitation of Fe(III) at high initial pH of the solution.

3.4.2. Influence of anions on FLT removal

For the PMS/Fe(II)/AA process, Figure S13a shows that FLT was removed 90.9, 100.0, and 87.0% with the concentrations of Cl^- increase from 1.0 to 50 mM, respectively. Analogously, FLT was removed 92.9, 74.0, and 73.1% in Figure S13b when the addition of Cl^- increased from 1.0 to 50 mM in the PMS/Fe(III)/AA system. It suggested that FLT removal was hardly affected by Cl^- and mildly increased with adding lesser dosages of Cl^-. It could be explained by the reasons below. Firstly, Cl^- could react with $SO_4^{\bullet-}$ (Equation (1) in Table 2), but the reaction is reversible (Yuan *et al.* 2011). As shown in Equations (1) and (3) (Table 2), the reaction between Cl^- and ROS could generate $Cl^{\cdot}$ (2.4 V) and $Cl_2^{\bullet-}$ (2.0 V) radicals, which could easily react with organic compounds (Yang *et al.* 2019). HOCl could be produced by the reaction of HSO_5^-, SO_5^{2-}, and Cl^- (Equations (4) and (5) in Table 2), which can accelerate the degradation of FLT (Zhou *et al.* 2018). In addition, $HO^{\bullet}$ could react with Cl^- causing unnecessary consumption (Equation (2) in Table 2), which was the reason why FLT removal mildly decreased with the dosage of Cl^- increasing to 50 mM (Baensch *et al.* 1991). The above results explained that FLT removal mildly increased with the small dosages of Cl^-.

Table 2 | Reactions and rate constants on different anions

Equation	Reaction	Rate constant	Ref.
1	$Cl^- + SO_4^{\bullet -} \leftrightarrow SO_4^{2-} + Cl^{\bullet}$	$k_f = (3.2 \pm 0.4) \times 10^8\ M^{-1}\ s^{-1}$, $k_r = (2.1 \pm 0.8) \times 10^8\ M^{-1}\ s^{-1}$	Yuan *et al.* (2011)
2	$Cl^- + HO^{\bullet} \leftrightarrow HOCl^{\bullet -}$	$k_f = (4.3 \pm 0.4) \times 10^{10}\ M^{-1}\ s^{-}$, $k_r = (6.1 \pm 0.8) \times 10^9\ M^{-1}\ s^{-1}$	Yuan *et al.* (2011)
3	$Cl^- + Cl^{\bullet} \leftrightarrow Cl_2^{\bullet -}$	$k_f = (7.8 \pm 0.8) \times 10^7\ M^{-1}\ s^{-1}$, $k_r = (5.7 \pm 0.4) \times 10^4\ M^{-1}\ s^{-1}$	Yuan *et al.* (2011)
4	$Cl^- + HSO_5^- \rightarrow SO_4^{2-} + HOCl$	$k = 2.06 \times 10^{-3}\ M^{-1}\ s^{-1}$	Zhou *et al.* (2018)
5	$Cl^- + SO_5^{2-} \rightarrow SO_4^{2-} + HOCl$	$k = 3.8 \times 10^{-4}\ M^{-1}\ s^{-1}$	Zhou *et al.* (2018)
6	$Br^- + SO_4^{\bullet -} \rightarrow SO_4^{2-} + Br^{\bullet}$	$k = 3.5 \times 10^9\ M^{-1}\ s^{-1}$	Wang *et al.* (2018)
7	$Br^- + HO^{\bullet} \leftrightarrow HOBr^{\bullet -}$	$k_f = 1.1 \times 10^{10}\ M^{-1}\ s^{-1}$, $k_r = 3.3 \times 10^7\ M^{-1}\ s^{-1}$	Wang *et al.* (2018)
8	$Br^{\bullet} + Br^{\bullet} \rightarrow Br_2$	$k = 1.0 \times 10^9\ M^{-1}\ s^{-1}$	Wang *et al.* (2018)
9	$Br^{\bullet} + Br^- \rightarrow Br_2^{\bullet -}$	$k_f = 1.0 \times 10^{10}\ M^{-1}\ s^{-1}$, $k_r = 1.0 \times 10^5\ M^{-1}\ s^{-1}$	Wang *et al.* (2018)
10	$Br_2^{\bullet -} + Br_2^{\bullet -} \rightarrow Br_2 + 2Br^-$	$k = 1.9 \times 10^9\ M^{-1}\ s^{-1}$	Wang *et al.* (2018)
11	$HCO_3^- + SO_4^{\bullet -} \rightarrow CO_3^{\bullet -} + SO_4^{2-} + H^+$	$k = 1.9 \times 10^9\ M^{-1}\ s^{-1}$	Lutze *et al.* (2015)
12	$HCO_3^- + HO^{\bullet} \rightarrow CO_3^{\bullet -} + OH^- + H^+$	$k = 1.9 \times 10^9\ M^{-1}\ s^{-1}$	Lutze *et al.* (2015)

In contrast to Cl^-, the degradation of FLT decreased to 14.1 and 11.5% with the concentrations of Br^- increasing to 50 mM for PMS/Fe(II)/AA and PMS/Fe(III)/AA processes. First of all, the abundant presence of Br^-, $SO_4^{\bullet -}$, and $HO^{\bullet}$ can largely be consumed through the reaction of Equations (6) and (7) in Table 2, which caused the reduction of ROS in solution to terminate FLT removal. What is more, the radicals ($Br^{\bullet}$ and $Br_2^{\bullet -}$) generated by the reaction of Br^- with ROS ($SO_4^{\bullet -}$ and $HO^{\bullet}$), further reacted with each other or themselves (Equations (8)–(10) in Table 2) to form Br_2 and released into the air.

As shown in Figure S13a and Figure S13b, FLT removal was immensely restricted following the concentrations of HCO_3^- increasing from 1.0 to 50 mM. For the PMS/Fe(II)/AA process, the degradation of FLT decreased from 90.0 to 47.6, 36.3, and 5.5% with the concentrations of HCO_3^- increasing from 0 to 50 mM. Similarly, FLT removal decreased from 91.8 to 38.6, 14.8, and 4.8% in the PMS/Fe(III)/AA system. The phenomenon can be explained in two ways. On the one hand, HCO_3^- could react with $SO_4^{\bullet -}$ and $HO^{\bullet}$ to decrease the content of ROS through the reaction of Equations (11) and (12) in Table 2. On the other hand, the solution pH was increased in Table S1 when the dosages increased from 1.0 to 50 mM, which caused Fe(II) and Fe(III) to precipitate. In conclusion, for selected three inorganic anions in this study, the presence of HCO_3^- has the largest effect on FLT removal in both systems.

3.5. Effect of humic acid on FLT removal

For PMS/Fe(II)/AA system, Figure 4(a) and 4(b) show that FLT removal mildly enhanced from 90.0 to 96.2% with the HA concentrations increasing to 3.0 mg L^{-1}, and increased from 91.8 to 100.0% in the PMS/Fe(III)/AA system. However, only 33.2 and 18.4% of FLT were removed in an aqueous solution containing 100 mg L^{-1} of HA for PMS/Fe(II)/AA and PMS/Fe(III)/AA processes. The reasons for lower FLT removal of higher concentrations of HA are as follows. First of all, the high HA concentrations could cause HA as a radical scavenger to compete with FLT for $SO_4^{\bullet -}$ and $HO^{\bullet}$ (Rajaei *et al.* 2021). The initial pH of the solution gradually increased with rising concentrations of HA in Table S1, which resulted in iron precipitates and reduced the content of dissolved iron. To sum up, the high concentrations of HA were unfavorable for FLT removal, and the effect of FLT removal was better in a limited HA range comparing the PMS/Fe(III)/AA process to the PMS/Fe(II)/AA process.

3.6. The efficiency of FLT degradation in the groundwater

Actual groundwater was selected instead of ultrapure water to study the efficiency of FLT in the actual groundwater in PMS/Fe(III)/AA and PMS/Fe(II)/AA processes, in which the substance contained is complex and the major characteristics are

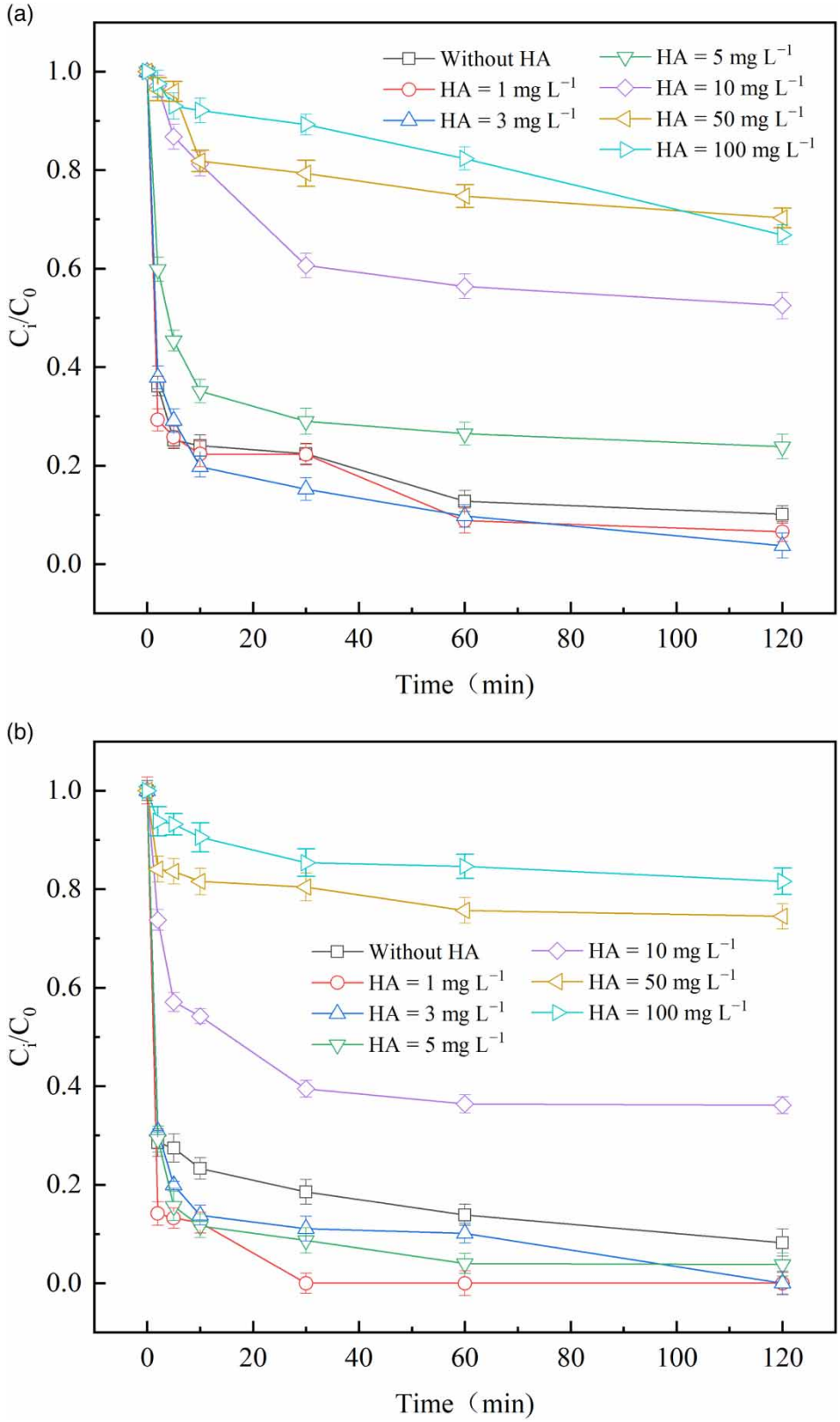

Figure 4 | Effect of HA on FLT degradation detected by HPLC in (a) PMS/Fe(II)/AA system ($[FLT]_0 = 0.2$ mg L^{-1}, $[PMS]_0 = 5.0$ mg L^{-1}, $[Fe(II)]_0 = 2.0$ mg L^{-1}, and $[AA]_0 = 2.8$ mg L^{-1}) and (b) PMS/Fe(III)/AA system ($[PMS]_0 = 12$ mg L^{-1}, $[FLT]_0 = 0.2$ mg L^{-1}, $[Fe(III)]_0 = 11$ mg L^{-1}, and $[AA]_0 = 3.5$ mg L^{-1}).

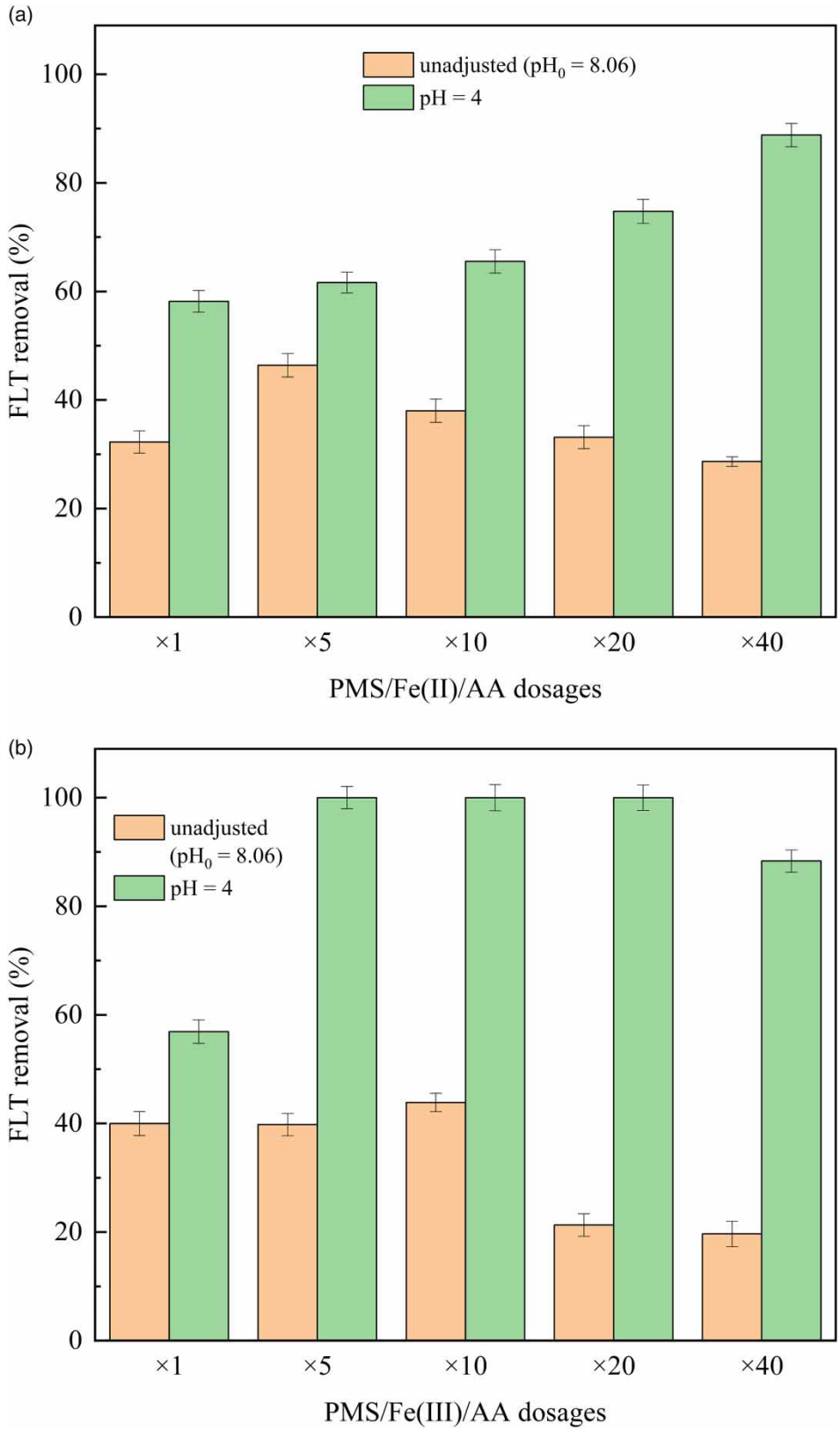

Figure 5 | FLT degradation performance in actual groundwater detected by HPLC in (a) PMS/Fe(II)/AA system ($[FLT]_0 = 0.2$ mg L^{-1}, $[PMS]_0 = 5.0$ mg L^{-1}, $[Fe(II)]_0 = 2.0$ mg L^{-1}, and $[AA]_0 = 2.8$ mg L^{-1}) and (b) PMS/Fe(III)/AA system ($[PMS]_0 = 12$ mg L^{-1}, $[FLT]_0 = 0.2$ mg L^{-1}, $[Fe(III)]_0 = 11$ mg L^{-1}, and $[AA]_0 = 3.5$ mg L^{-1}).

displayed in Table S2. Figure 5(a) and 5(b) show that FLT only removed 32.3 and 40.0% in the natural groundwater without pH adjustment when the dosages of PMS/Fe(II)/AA/FLT and PMS/Fe(III)/AA/FLT were set to 2/2/4/1 and 5/10/5/1, which FLT removal was significantly lower than the ultrapure water, respectively. FLT removal increased when the chemical dosages of both systems extended to 5, 10, 20, and 40-fold, respectively. There are several reasons for this phenomenon. On the one hand, FLT removal was declined because the high pH of the solution resulted in the formation of Fe(II) and Fe(III) precipitates. On the other hand, the actual groundwater (contains a high concentration of HCO_3^-) has a powerful buffering capacity, and HCO_3^- could consume the ROS of the solution to hold back FLT removal. Therefore, for the PMS/Fe(II)/AA process, the degradation of FLT increased from 58.2 to 61.6, 65.5, 74.8, and 88.8% with the chemical dosages to 1, 5, 10, 20, and 40-fold when the pH of groundwater was pre-adjusted to 4.0 by 0.1 M H_2SO_4, respectively. Similarly, FLT removal increased from 56.9 to 100, 100, 100, and 88.3% in the PMS/Fe(III)/AA process, respectively. It indicated that the adverse effects were effectively overcome through pH adjustment in the practical application of groundwater remediation. The prices of industrial-grade reagents such as PMS, Fe(II), Fe(III), and AA were about 3.3, 0.3, 0.6, and 17 RMB/kg, respectively. In actual groundwater remediation, the dosages of PMS, Fe(II), and AA were 0.2, 0.08, and 0.11 g L^{-1}, respectively, for the PMS/Fe(II)/AA system. Meanwhile, for the PMS/Fe(III)/AA system, the dosages of PMS, Fe(II), and AA were 0.06, 0.06, and 0.02 g L^{-1}, respectively. Therefore, the cost of remediating actual groundwater contaminated by FLT was 2.55 and 0.57 RMB for PMS/Fe(II)/AA and PMS/Fe(III)/AA systems based on 1.0 m^3 of water, which was acceptable for actual remediation. The adverse effects of the pH decline can be reduced by the addition of naturally occurring alkaline substances such as lime (Anhua *et al.* 2014). The presence of other contaminants or degradation intermediates can inhibit the degradation of FLT due to the competitive effect with FLT for the ROS generated in PMS systems (Huang *et al.* 2017; Cao *et al.* 2019; Yang *et al.* 2019; Li *et al.* 2019a; Luo *et al.* 2021; Dong *et al.* 2021). To our delight, the above negative effects could be overcome by increasing proportionally the dosage of the chemicals in the actual groundwater degradation, thereby promoting FLT removal.

Sheng *et al.* (2022) investigated the degradation effect of sodium percarbonate (SPC)/Fe(II) system on FLT, and 90.3% of FLT in the actual groundwater was degraded after 15 min of reaction when the dosages of SPC, Fe(II) were 0.15 and 1 mM, respectively. In this study, for the PMS/Fe(II)/AA system, the degradation of FLT was 74.8% after 120 min when the dosages

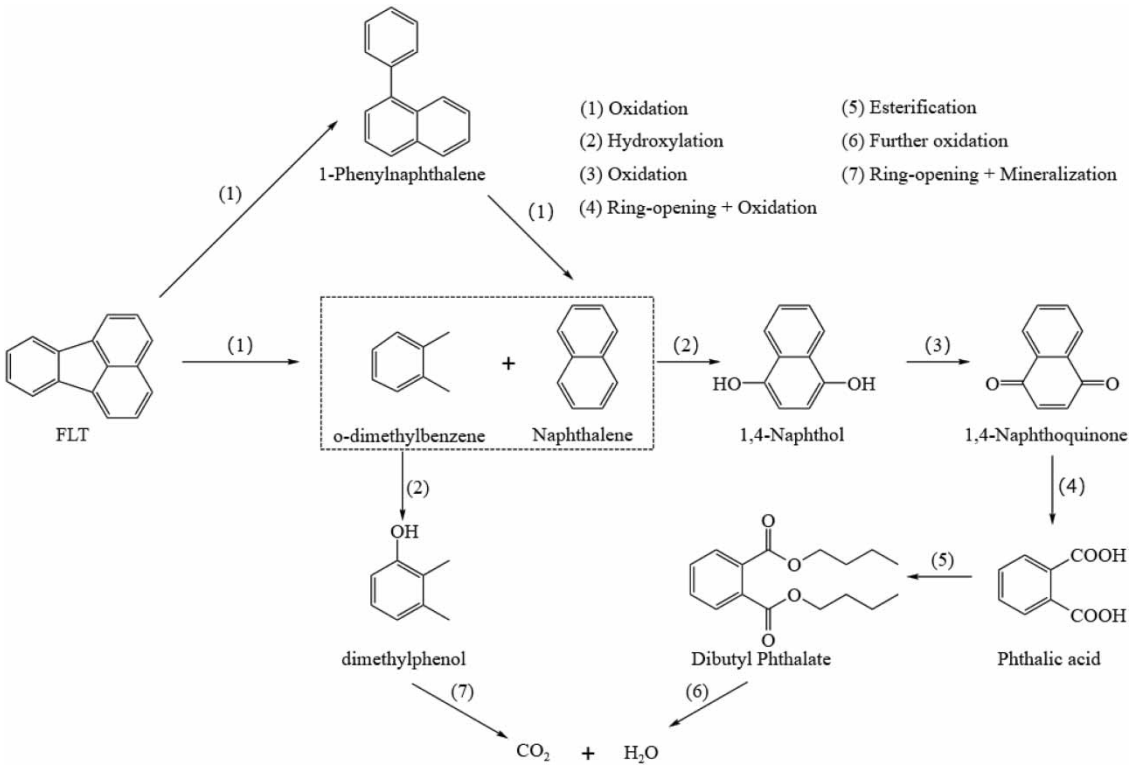

Figure 6 | Degradation pathways of FLT in PMS/Fe(II)/AA and PMS/Fe(III)/AA systems detected by GC–MS.

of PMS, Fe(II), and AA were 0.04, 0.04, and 0.16 mM, respectively. For the PMS/Fe(III)/AA system, the FLT degradation rate was 100% after 120 min when the dosages of PMS, Fe(III), and AA were 0.025, 0.05, and 0.025 mM, respectively. The above comparisons demonstrated that the PMS/Fe(II)/AA and PMS/Fe(III)/AA systems used significantly less reagent than the previously studied methods, implying that the AA-enhanced technology presents some advantages for the remediation of FLT contamination. Besides, most of the reagents used in the above research were procured from Macklin Biochemical Co. Ltd (Shanghai, China) and Aladdin Reagent Co. Ltd (Shanghai, China), PMS was about twice as expensive as SPC, Fe(III) and Fe(II) were about the same price. In conclusion, degradation of FLT using AA enhancement technology was more economical compared to previous studies.

3.7. Possible FLT removal pathways

Table S3 shows the intermediates of FLT removal analyzed by GC–MS in PMS/Fe(II)/AA and PMS/Fe(III)/AA processes, and chromatograms are supplied in Figure S14. For PMS/Fe(II)/AA process, the detected intermediates are similar to PMS/Fe(III)/AA process, and the probable pathways of FLT removal were proposed based on GC–MS analytical results and other research (Zeng *et al.* 2022; Zhu *et al.* 2022). The primary pathways of FLT removal were speculated on the basis of the detected intermediate products in Figure 6. First of all, FLT was converted to 1-phenyl naphthalene or *o*-dimethylbenzene (*o*-xylene) and naphthalene through thermal cracking, and 1-phenyl naphthalene was also further cracked to naphthalene through oxidation. Secondly, naphthalene was attacked by $HO^{\bullet}$ to produce 1,4-naphthol, and dimethylphenol was generated by the hydroxylation of *o*-xylene. Then, 1,4-naphthoquinone was formed under the continued oxidation of 1,4-naphthol. Furthermore, phthalic anhydride was produced by the ring-opening of 1,4-naphthoquinone. In addition, phthalic acid was further esterificated to dibutyl phthalate through esterification. Finally, dimethylphenol and dibutyl phthalate were further transformed to CO_2 and H_2O after complete mineralization. As shown in Table S4, the toxicity of FLT degradation intermediates detected by GC-MC was calculated by the TEST tool. The LD50 of FLT was lower than the detected intermediates, indicating that the processes of FLT removal by PMS/Fe(II)/AA and PMS/Fe(III)/AA systems were both environmentally friendly.

4. CONCLUSIONS

In this study, the addition of AA significantly enhanced the degradation of FLT in PMS/Fe(II) and PMS/Fe(III) systems with molar ratios of 2/2/4 and 5/10/5 for PMS/Fe(II)/AA and PMS/Fe(III)/AA systems, respectively. It was elaborated that the degradation of FLT was enhanced by promoting the production of ROS due to the reduction and chelation of AA through the detection of Fe(II) concentration and the demonstration experiments of chelated iron. For PMS/Fe(II)/AA and PMS/Fe(III)/AA systems, the results from the probe and scavenging experiments suggested that $SO_4^{\bullet-}$ was the dominant ROS for FLT removal. The validation and comparison of the effects of both systems on the degradation of FLT under different groundwater matrixes indicated that the PMS/Fe(III)/AA system had better adaptability than the PMS/Fe(II)/AA system. The intermediates of FLT degradation, such as 1-phenylnaphthalene, o-xylene, dibutyl phthalate, and naphthalene, were detected by GC–MS, and the possible pathways of FLT degradation were proposed. In the actual groundwater degradation experiments, the degradation rates of FLT in the PMS/Fe(II)/AA and PMS/Fe(III)/AA systems reached 88.8 and 100.0%, respectively, and the dosage of chemicals in PMS/Fe(III)/AA system was less than that required in PMS/Fe(II)/AA system due to the better adaptability of PMS/Fe(III)/AA system for different water conditions.

ACKNOWLEDGEMENTS

This study was financially supported by a grant from the National Natural Science Foundation of China (No. 41977164).

DATA AVAILABILITY STATEMENT

All relevant data are included in the paper or its Supplementary Information.

CONFLICT OF INTEREST

The authors declare there is no conflict.

REFERENCES

Ahmad, M., Teel, A. L., Furman, O. S., Reed, J. I. & Watts, R. J. 2012 Oxidative and reductive pathways in iron-ethylenediaminetetraacetic acid-activated persulfate systems. *Journal of Environmental Engineering* **138** (4), 411–418. https://doi.org/10.1061/(ASCE)EE.1943-7870.0000496.

Ahmad, A., Gu, X., Li, L., Lu, S., Xu, Y. & Guo, X. 2015 Effects of pH and anions on the generation of reactive oxygen species (ROS) in nZVI-rGO-activated persulfate system. *Water, Air, & Soil Pollution* **226** (11), 369. https://doi.org/10.1007/s11270-015-2635-8.

Anhua, L., Yang, L. & Hui, Z. 2014 In situ chemical oxidation of organic contaminated soil and groundwater using activated persulfate process. *Progress in Chemistry* **26** (05), 898. https://doi.org/10.7536/PC130952.

Anipsitakis, G. P. & Dionysiou, D. D. 2004 Radical generation by the interaction of transition metals with common oxidants. *Environmental Science & Technology* **38** (13), 3705–3712. https://doi.org/10.1021/es035121o.

Baensch, B., Martinez, P., Uribe, D., Zuluaga, J. & Van Eldik, R. 1991 Is the oxidation of L-ascorbic acid by aquated iron(III) ions in acidic aqueous solution substitution or electron-transfer-controlled a combined chloride, pH, temperature, and pressure dependence study. *Inorganic Chemistry* **30** (24), 4555–4559. https://doi.org/10.1021/ic00024a018.

Bein, E., Seiwert, B., Reemtsma, T., Drewes, J. E. & Hübner, U. 2023 Advanced oxidation processes for removal of monocyclic aromatic hydrocarbon from water: Effects of O_3/H_2O_2 and UV/H_2O_2 treatment on product formation and biological post-treatment. *Journal of Hazardous Materials* **450**, 131066. https://doi.org/10.1016/j.jhazmat.2023.131066.

Buxton, G. V., Greenstock, C. L., Helman, W. P. & Ross, A. B. 1988 Critical review of rate constants for reactions of hydrated electrons, hydrogen atoms and hydroxyl radicals ($\cdot OH/\cdot O^-$) in aqueous solution. *Journal of Physical and Chemical Reference Data* **17** (2), 513–886. https://doi.org/10.1063/1.555805.

Cao, J., Lai, L., Lai, B., Yao, G., Chen, X. & Song, L. 2019 Degradation of tetracycline by peroxymonosulfate activated with zero-valent iron: Performance, intermediates, toxicity and mechanism. *Chemical Engineering Journal* **364**, 45–56. https://doi.org/10.1016/j.cej.2019.01.113.

Carol, E. & Alvarez, M. D. P. 2016 Processes regulating groundwater chloride content in marshes under different environmental conditions: A comparative case study in Península Valdés and Samborombón Bay, Argentina. *Continental Shelf Research* **115**, 33–43. https://doi.org/10.1016/j.csr.2015.12.017.

Chan, K. H. & Chu, W. 2009 Degradation of atrazine by cobalt-mediated activation of peroxymonosulfate: Different cobalt counteranions in homogenous process and cobalt oxide catalysts in photolytic heterogeneous process. *Water Research* **43** (9), 2513–2521. https://doi.org/10.1016/j.watres.2009.02.029.

Cheng, M., Zeng, G., Huang, D., Lai, C., Xu, P., Zhang, C. & Liu, Y. 2016 Hydroxyl radicals based advanced oxidation processes (AOPs) for remediation of soils contaminated with organic compounds: A review. *Chemical Engineering Journal* **284**, 582–598. https://doi.org/10.1016/j.cej.2015.09.001.

Davies, M. B. 1992 Reactions of L-ascorbic acid with transition metal complexes. *Polyhedron* **11** (3), 285–321. https://doi.org/10.1016/S0277-5387(00)83175-7.

Dong, H., Xu, Q., Lian, L., Li, Y., Wang, S., Li, C. & Guan, X. 2021 Degradation of organic contaminants in the Fe(II)/peroxymonosulfate process under acidic conditions: The overlooked rapid oxidation stage. *Environmental Science & Technology* **55** (22), 15390–15399. https://doi.org/10.1021/acs.est.1c04563.

Fang, G., Dionysiou, D., Al-Abed, S. & Zhou, D. 2013 Superoxide radical driving the activation of persulfate by magnetite nanoparticles: Implications for the degradation of PCBs. *Applied Catalysis B: Environmental* **129**, 325–332. https://doi.org/10.1016/j.apcatb.2012.09.042.

Huang, G., Wang, C., Yang, C., Guo, P. & Yu, H. 2017 Degradation of bisphenol a by peroxymonosulfate catalytically activated with $Mn_{1.8}Fe_{1.2}O_4$ nanospheres: Synergism between Mn and Fe. *Environmental Science & Technology* **51** (21), 12611–12618. https://doi.org/10.1021/acs.est.7b03007.

Kontoghiorghes, G. J., Kolnagou, A., Kontoghiorghe, C. N., Mourouzidis, L., Timoshnikov, V. A. & Polyakov, N. E. 2020 Trying to solve the puzzle of the interaction of ascorbic acid and iron: Redox, chelation and therapeutic implications. *Medicines* **7** (8), 45. https://doi.org/10.3390/medicines7080045.

Li, J., Xu, M., Yao, G. & Lai, B. 2018a Enhancement of the degradation of atrazine through $cofe_2o_4$ activated peroxymonosulfate (PMS) process: Kinetic, degradation intermediates, and toxicity evaluation. *Chemical Engineering Journal* **348**, 1012–1024. https://doi.org/10.1016/j.cej.2018.05.032.

Li, X., Huang, X., Xi, S., Miao, S., Ding, J., Cai, W., Liu, S., Yang, X., Yang, H., Gao, J., Wang, J., Huang, Y., Zhang, T. & Liu, B. 2018b Single cobalt atoms anchored on porous N-doped graphene with dual reaction sites for efficient Fenton-like catalysis. *Journal of the American Chemical Society* **140** (39), 12469–12475. https://doi.org/10.1021/jacs.8b05992.

Li, J., Wan, Y., Li, Y., Yao, G. & Lai, B. 2019a Surface Fe(III)/Fe(II) cycle promoted the degradation of atrazine by peroxymonosulfate activation in the presence of hydroxylamine. *Applied Catalysis B: Environmental* **256**, 117782. https://doi.org/10.1016/j.apcatb.2019.117782.

Li, L., Lai, C., Huang, F., Cheng, M., Zeng, G., Huang, D. & Li, B. 2019b Degradation of naphthalene with magnetic bio-char activate hydrogen peroxide: Synergism of bio-char and Fe-Mn binary oxides. *Water Research* **160**, 238–248. https://doi.org/10.1016/j.watres.2019.05.081.

Li, X., Wu, B., Zhang, Q., Xu, D., Liu, Y., Ma, F. & Gu, Q. 2019c Mechanisms on the impacts of humic acids on persulfate/Fe(II)-based groundwater remediation. *Chemical Engineering Journal* **378**, 122142. https://doi.org/10.1016/j.cej.2019.122142.

Li, Y., Dong, H., Xiao, J., Li, L., Hou, Y., Chu, D. & Hou, X. 2023 Ascorbic acid-assisted iron silicate composite activated peroxydisulfate for enhanced degradation of aqueous contaminants: Accelerated Fe(III)/Fe(II) cycle and the interaction between iron and silicate. *Chemical Engineering Journal* **455**, 140773. https://doi.org/10.1016/j.cej.2022.140773.

Lim, J., Lee, J., Kim, C., Hwang, S., Lee, J. & Choi, W. 2019 Two-dimensional RuO_2 nanosheets as robust catalysts for peroxymonosulfate activation. *Environmental Science: Nano* **6** (7), 2084–2093. https://doi.org/10.1039/C9EN00500E.

Long, X., Xiong, Z., Huang, R., Yu, Y., Zhou, P., Zhang, H. & Yao, G. 2022 Sustainable Fe(III)/Fe(II) cycles triggered by co-catalyst of weak electrical current in Fe(III)/peroxymonosulfate system: Collaboration of radical and non-radical mechanisms. *Applied Catalysis B: Environmental* **317**, 121716. https://doi.org/10.1016/j.apcatb.2022.121716.

Luo, H., Zeng, Y., Cheng, Y., He, D. & Pan, X. 2021 Activation of peroxymonosulfate by iron oxychloride with hydroxylamine for ciprofloxacin degradation and bacterial disinfection. *Science of The Total Environment* **799**, 149506. https://doi.org/10.1016/j.scitotenv.2021.149506.

Lutze, H. V., Kerlin, N. & Schmidt, T. C. 2015 Sulfate radical-based water treatment in presence of chloride: Formation of chlorate, interconversion of sulfate radicals into hydroxyl radicals and influence of bicarbonate. *Water Research. Occurrence, Fate, Removal and Assessment of Emerging Contaminants in Water in the Water Cycle (From Wastewater to Drinking Water* **72**, 349–360. https://doi.org/10.1016/j.watres.2014.10.006.

Lyu, Y., Lyu, S., Tang, P., Jiang, W., Sun, Y., Li, M. & Sui, Q. 2020 Degradation of trichloroethylene in aqueous solution by sodium percarbonate activated with Fe(II)-citric acid complex in the presence of surfactant Tween-80. *Chemosphere* **257**, 127223. https://doi.org/10.1016/j.chemosphere.2020.127223.

Munialo, C. D. & Kontogiorgos, V. 2014 An investigation into the degradation of ascorbic acid in solutions. *International Journal of Food Science And Technology* **2** (3), 106–112.

Pignatello, J. J., Oliveros, E. & MacKay, A. 2006 Advanced oxidation processes for organic contaminant destruction based on the Fenton reaction and related chemistry. *Critical Reviews in Environmental Science and Technology* **36** (1), 1–84. https://doi.org/10.1080/10643380500326564.

Rajaei, F., Taheri, E., Hadi, S., Fatehizadeh, A., Amin, M. M., Rafei, N. & Fadaei, S. 2021 Enhanced removal of humic acid from aqueous solution by combined alternating current electrocoagulation and sulfate radical. *Environmental Pollution* **277**, 116632. https://doi.org/10.1016/j.envpol.2021.116632.

Rastogi, A., Al-Abed, S. R. & Dionysiou, D. D. 2009a Effect of inorganic, synthetic and naturally occurring chelating agents on Fe(II) mediated advanced oxidation of chlorophenols. *Water Research* **43** (3), 684–694. https://doi.org/10.1016/j.watres.2008.10.045.

Rastogi, A., Al-Abed, S. R. & Dionysiou, D. D. 2009b Sulfate radical-based ferrous-peroxymonosulfate oxidative system for PCBs degradation in aqueous and sediment systems. *Applied Catalysis B: Environmental* **85** (3–4), 171–179. https://doi.org/10.1016/j.apcatb.2008.07.010

Ren, H., Jin, X., Li, C., Li, T., Liu, Y. & Zhou, R. 2020 Rosmarinic acid enhanced Fe(III)-mediated Fenton oxidation removal of organic pollutants at near neutral pH. *Science of the Total Environment* **736**, 139528. https://doi.org/10.1016/j.scitotenv.2020.139528.

Roig, M. G., Rivera, Z. S. & Kennedy, J. F. 1993 L-ascorbic acid: An overview. *International Journal of Food Sciences and Nutrition* **44** (1), 59–72. https://doi.org/10.3109/09637489309017424.

Sheng, X., Xu, Z., Liu, Y., Wang, P., Dong, J., Lu, Z., Shan, A. & Lyu, S. 2022 Fluoranthene removal in aqueous phase by Fe(II) activated sodium percarbonate: Mechanisms and degradation pathways. *Research on Chemical Intermediates* **48** (4), 1645–1663. https://doi.org/10.1007/s11164-021-04624-2.

Sunder, M. & Hempel, D. 1997 Oxidation of tri- and perchloroethene in aqueous solution with ozone and hydrogen peroxide in a tube reactor. *Water Research* **31** (1), 33–40. https://doi.org/10.1016/S0043-1354(96)00218-7.

Sutton, N. B., Grotenhuis, J. T. C., Langenhoff, A. A. M. & Rijnaarts, H. H. M. 2011 Efforts to improve coupled in situ chemical oxidation with bioremediation: A review of optimization strategies. *Journal of Soils and Sediments* **11** (1), 129–140. https://doi.org/10.1007/s11368-010-0272-9.

Teel, A. L. & Watts, R. J. 2002 Degradation of carbon tetrachloride by modified Fenton's reagent. *Journal of Hazardous Materials* **94** (2), 179–189. https://doi.org/10.1016/S0304-3894(02)00068-7.

Thinh, N. V., Osanai, Y., Adachi, T., Vuong, B. T. S., Kitano, I., Chung, N. T. & Thai, P. K. 2021 Removal of lead and other toxic metals in heavily contaminated soil using biodegradable chelators: GLDA, citric acid and ascorbic acid. *Chemosphere* **263**, 127912. https://doi.org/10.1016/j.chemosphere.2020.127912.

Torres, R., Blesa, M. & Matijević, E. 1982 Interactions of metal hydrous oxides with chelating agents: IX. reductive dissolution of hermatite and magnetite by aminocarboxylic acids. *Journal of Colloid and Interface Science* **134**, 475–485. https://doi.org/10.1016/0021-9797(90)90157-J.

Tripathi, R., Singh, B., Bisht, S. & Pandey, J. 2009 L-ascorbic acid in organic synthesis: An overview. *Current Organic Chemistry* **13** (1), 99–122. https://doi.org/10.2174/138527209787193792.

Tu, Y., Njus, D. & Schlegel, H. 2017 A theoretical study of ascorbic acid oxidation and $HOO^{\cdot}/O_2^{\cdot-}$ radical scavenging. *Organic & Biomolecular Chemistry* **15** (20), 4417–4431. https://doi.org/10.1039/C7OB00791D.

Wang, J. & Wang, S. 2018 Activation of persulfate (PS) and peroxymonosulfate (PMS) and application for the degradation of emerging contaminants. *Chemical Engineering Journal* **334**, 1502–1517. https://doi.org/10.1016/j.cej.2017.11.059.

Wang, S., Sheng, Y., Feng, M., Leszczynski, J., Wang, L., Tachikawa, H. & Yu, H. 2007 Light-induced cytotoxicity of 16 polycyclic aromatic hydrocarbons on the US EPA priority pollutant list in human skin HaCaT keratinocytes: Relationship between phototoxicity and excited state properties. *Environmental Toxicology* **22** (3), 318–327. https://doi.org/10.1002/tox.20241.

Wang, L., Kong, D., Ji, Y., Lu, J., Yin, X. & Zhou, Q. 2018 Formation of halogenated disinfection byproducts during the degradation of chlorophenols by peroxymonosulfate oxidation in the presence of bromide. *Chemical Engineering Journal* **343**, 235–243. https://doi.org/10.1016/j.cej.2018.03.006.

Wu, X., Gu, X., Lu, S., Xu, M., Zang, X., Miao, Z. & Qiu, Z. 2014 Degradation of trichloroethylene in aqueous solution by persulfate activated with citric acid chelated ferrous ion. *Chemical Engineering Journal* **255**, 585–592. https://doi.org/10.1016/j.cej.2014.06.085.

Wu, X., Gu, X., Lu, S., Qiu, Z., Sui, Q., Zang, X. & Miao, Z. 2015 Strong enhancement of trichloroethylene degradation in ferrous ion activated persulfate system by promoting ferric and ferrous ion cycles with hydroxylamine. *Separation and Purification Technology* **147**, 186–193. https://doi.org/10.1016/j.seppur.2015.04.031.

Xu, X., Li, X., Li, X. & Li, H. 2009 Degradation of melatonin by UV, UV/H_2O_2, Fe^{2+}/H_2O_2 and UV/Fe^{2+}/H_2O_2 processes. *Separation and Purification Technology* **68** (2), 261–266. https://doi.org/10.1016/j.seppur.2009.05.013.

Xu, P., Wang, L., Liu, X., Xie, S., Yang, Z. & Zhu, P. 2022 Ascorbic acid enhanced the zero-valent iron/peroxymonosulfate oxidation: Simultaneous chelating and reducing. *Separation and Purification Technology* **298**, 121599. https://doi.org/10.1016/j.seppur.2022.121599.

Yang, Y., Banerjee, G., Brudvig, G., Kim, J. & Pignatello, J. 2018 Oxidation of organic compounds in water by unactivated peroxymonosulfate. *Environmental Science & Technology* **52** (10), 5911–5919. https://doi.org/10.1021/acs.est.8b00735.

Yang, Y., Cao, Y., Jiang, J., Lu, X., Ma, J., Pang, S. & Li, J. 2019 Comparative study on degradation of propranolol and formation of oxidation products by UV/H_2O_2 and UV/persulfate (PDS). *Water Research* **149**, 543–552. https://doi.org/10.1016/j.watres.2018.08.074.

Yuan, R., Ramjaun, S. N., Wang, Z. & Liu, J. 2011 Effects of chloride ion on degradation of acid orange 7 by sulfate radical-based advanced oxidation process: Implications for formation of chlorinated aromatic compounds. *Journal of Hazardous Materials* **196**, 173–179. https://doi.org/10.1016/j.jhazmat.2011.09.007.

Zeng, G., Yang, R., Zhou, Z., Huang, J., Danish, M. & Lyu, S. 2022 Insights into naphthalene degradation in aqueous solution and soil slurry medium: Performance and mechanisms. *Chemosphere* **291**, 132761. https://doi.org/10.1016/j.chemosphere.2021.132761.

Zhang, P. & Chen, Y. 2017 P Polycyclic aromatic hydrocarbons contamination in surface soil of China: A review. *Science of The Total Environment* **605–606**, 1011–1020. https://doi.org/10.1016/j.scitotenv.2017.06.247.

Zhou, P., Zhang, J., Zhang, Y., Liu, Y., Liang, J., Liu, B. & Zhang, W. 2016 Generation of hydrogen peroxide and hydroxyl radical resulting from oxygen-dependent oxidation of L-ascorbic acid via copper redox-catalyzed reactions. *RSC Advances* **6** (45), 38541–38547. https://doi.org/10.1039/C6RA02843H.

Zhou, Y., Jiang, J., Gao, Y., Pang, S., Ma, J., Duan, J. & Guo, Q. 2018 Oxidation of steroid estrogens by peroxymonosulfate (PMS) and effect of bromide and chloride ions: Kinetics, products, and modeling. *Water Research* **138**, 56–66. https://doi.org/10.1016/j.watres.2018.03.045.

Zhu, Y., Ji, S., Liang, W., Li, C., Nie, Y., Dong, J. & Shi, W. 2022 A low-cost and eco-friendly powder catalyst: Iron and copper nanoparticles supported on biochar/geopolymer for activating potassium peroxymonosulfate to degrade naphthalene in water and soil. *Chemosphere* **303**, 135185. https://doi.org/10.1016/j.chemosphere.2022.135185.

Zou, J., Ma, J., Chen, L., Li, X., Guan, Y., Xie, P. & Pan, C. 2013 Rapid acceleration of ferrous iron/peroxymonosulfate oxidation of organic pollutants by promoting Fe(III)/Fe(II) cycle with hydroxylamine. *Environmental Science & Technology* **47** (20), 11685–11691. https://doi.org/10.1021/es4019145.

First received 31 October 2023; accepted in revised form 11 March 2024. Available online 26 March 2024